Journal of Materials Chemistry B

PAPER

View Article Online
View Journal | View Issue

Cite this: J. Mater. Chem. B, 2014, 2, 7910

pH-controlled delivery of curcumin from a compartmentalized solid lipid nanoparticle@mesostructured silica matrix†

Sanghoon Kim, Marie-José Stébé, Jean-Luc Blin and Andreea Pasc*

Received 10th July 2014
Accepted 19th September 2014

DOI: 10.1039/c4tb01133c

www.rsc.org/MaterialsB

Silicalization of curcumin-loaded solid lipid nanoparticle (SLN)/micelle dispersions afforded a compartmentalized nanovector, with both macro- and mesostructured domains. SLNs act as reservoirs of curcumin (CU), while mesopores act as pathways to control drug release. Moreover, the release sustainability depends on the nature of the solid lipid (cetyl palmitate *vs.* stearic acid) and on the pH of the receiving phase. The meso–macrostructured silica matrix templated by SLNs appears thus as a promising drug delivery system for pH-responsive controlled release.

Introduction

In recent years, design of nanocarriers for controlled and sustained delivery of drugs has been extensively studied to overcome several problems in conventional drug delivery systems, such as poor solubility, limited stability and lack of selectivity of drugs.[1] Since the first application of the mesoporous silica nanoparticle (MSN) as a drug delivery system,[2] the MSN has attracted a lot of attention due to its large surface area, ordered mesopore structure, and good stability and also because its surface can be simply functionalized for drug loading.[3] Moreover, silica prepared by sol–gel has good biocompatibility within a certain range of administrated dose, approved by the US Food and Drug Administration or European Medicines Agency (EMA).[4] Therefore, numerous nanocarriers based on ordered mesoporous silica have been proposed, not only to improve drug encapsulation/release ability,[5] but also to build a smart delivery system that respond to external stimuli such as pH,[6] temperature[7] and magnetic field.[8] However, most methods involve multi-step synthesis and are relatively complex, especially during the drug loading step.[9] To overcome these disadvantages, the use of amphiphilic molecules as a structure-directing agent for building mesoporous silica and a drug encapsulating agent at the same time has been considered as a good alternative to overcome problems related to post-synthesis for drug loading. For instance, the hydrophobic drug can be easily loaded into the core of cetyltrimethylammonium bromide (CTAB) micelle and the presence of drug does not alter the formation of ordered mesoporous hybrid-silica.[10] An ibuprofen loaded alkyl maltoside surfactant was also used in the same manner.[11] However, the synthesis conditions (extremely low pH or an organic solvent like hexane) might limit the wide use of this method for chemically sensitive drugs and biological applications. In the organic matter field, solid lipid nanoparticles (SLNs) appeared as promising drug delivery carriers in the pharmaceutical field with an excellent biocompatibility.[12] SLNs that already contain certain amount of surfactants as stabilizing agents can be used directly to build hierarchical meso–macroporous silica materials as our group reported previously.[13] Moreover, because the synthesis takes place without adding hazardous acid, the use of SLNs as drug loading agents and meso–macropore templates appears to be a straightforward approach for the development of novel hybrid organic–inorganic biocompatible materials with high potential applications in drug delivery.

On another hand, curcumin (CU), a hydrophobic natural polyphenol isolated from *Curcuma longa*, has been used for centuries in indigenous medicine for the treatment of a variety of inflammatory conditions.[14] It exhibits a wide range of pharmacological capacities, including antitumor, antioxidant, anti-inflammatory, and antimicrobial activities.[15] Its most interesting potential use is probably against cancer: pre-clinical studies have shown that it can inhibit cancerogenesis in a variety of cell lines, including breast, cervical, colon, gastric, hepatic, oral epithelial, ovarian, pancreatic, prostate cancer and leukemia.[16] In addition, it was reported that CU caused cell death in eight melanoma cell lines, also in those carrying mutant p53, which are very resistant to conventional chemotherapy.[17] The main drawbacks for clinical applications of CU are its low water solubility at acidic and physiological pH and its rapid hydrolysis under alkaline conditions to yield ferulic acid, its methyl ester and vanillin.[18] It is also very susceptible to photochemical degradation.[19] Moreover, studies on its

Université de Lorraine, SRSMC, UMR 7565, F-54506 Vandoeuvre-lès-Nancy, Cedex, France. E-mail: andreea.pasc@univ-lorraine.fr; Tel: +33 383684344

† Electronic supplementary information (ESI) available: Full scale FT-IR spectra and SAXS diffractograms, fitting graphs using the Korsmeyer–Peppas model as well as solid lipid nanoparticle tracking analysis obtained with a nanoSight (Malvern). See DOI: 10.1039/c4tb01133c

absorption, distribution, metabolism and excretion have revealed that its poor absorption and rapid metabolism severely curtail its bioavailability.[20] These hurdles can be avoided by incorporating CU into nanoparticles, liposomes, and micelles, complexing it with cyclodextrins (CD) in aqueous solutions[21] or mesoporous silica.[22] Solid lipid nanoparticles (SLNs) loaded with CU for topical administration were also developed and characterized.[23] SLNs with a mean size of 450 nm were found to be stable for 6 months and incorporation into SLNs strongly reduced the light and oxygen sensitivity of curcuminoids. However, the organic matter based drug carriers could be physico-chemically instable, thus unexpected drug leaking can occur during storage.[24]

Herein, we designed a novel drug delivery system aimed to increase the stability, bioavailability and sustainability of the release of CU, through a double encapsulation of the drug into a core–shell nanomatrix combining SLNs and mesostructured silica. The SLN and hybrid materials were characterized by various techniques, including small-angle X-ray scattering (SAXS), N_2 adsorption–desorption, mercury porosimetry, and scanning and transmission electron microscopies (SEM and TEM). *In vitro* curcumin release from hybrid meso–macroporous silica materials was also tested at three different pH values (1.2, 4.5 and 7.2). The designed materials have potential *in vivo* applications since, except NHP, all ingredients are excipient for medicines and are listed as approved drug products by the FDA.[25]

Materials and methods

Materials

Tetramethylorthosilicate (TMOS), Pluronic P123, curcumin, hexadecyltrimethylammonium bromide (CTAB), sodium chloride, acetic acid, sodium acetate, potassium chloride, monopotassium phosphate and disodium phosphate were purchased from Sigma-Aldrich. Stearic acid (SA) and N-hexadecylpalmitate (NHP) were purchased from ACROS. Water was deionized using a Milli-Q pack system. All chemicals were used as received without further purification. All buffer solutions were prepared according to the methods described in the U.S. Pharmacopeia (USP 35-NF30).

SLN preparation

Curcumin-loaded solid lipid nanoparticles (CU-Lipid-SLNs) were prepared by ultra-sonication of a hot emulsion obtained from a mixture of curcumin and a melted lipid dispersed in a micellar phase.[26] In a typical procedure, the mixture of 2.2 g of solid lipid (SA or NHP) and 22 mg of curcumin was heated at 70–80 °C in an oil bath. The aqueous phase (6.9 wt% of P123) was heated at the same temperature as the lipid phase. The oil phase was added to 10 mL of the P123 micellar solution and the mixture was sonicated for 3 min with an ultrasonic device (Branson Sonifier, 40 W output power). The hot o/w emulsion was then cooled to room temperature under vigorous string to afford lipid solidification. The resulting CU-Lipid-SLNs are dispersed into a micellar solution of P123 and further used without phase separation. SLNs prepared from NHP and SA are denoted as CU-NHP-SLNs and CU-SA-SLNs, respectively.

Synthesis of hybrid SLN–silica materials

Silica materials were synthesized as previously reported by our group.[13] In a typical procedure, 900 mg of tetramethoxysilane (TMOS) was added dropwise under stirring at room temperature to 4 mL dispersion of CU-Lipid-SLNs into a micellar phase of P123. The surfactant/silica molar ratio (R) was 0.008. The mixture was stirred for 1 hour and then transferred into sealed Teflon autoclaves for hydrothermal treatment, which was assayed at 70 °C for 24 h. After the hydrothermal treatment, the material was dried at 40 °C for 7 days to evaporate water and residual methanol. The material prepared from CU-NHP-SLN and CU-SA-SLN is denoted as NHP-Mat and SA-Mat.

Characterization

SAXS measurements were carried out using a SAXSess mc^2 (Anton Paar) apparatus.[27] Transmission electron microscopy (TEM) analysis was performed using a Philips CM200 microscope, operating at an accelerating voltage of 200 kV. Scanning electron microscopy (SEM) was carried out with a HITACHI S-2500. N_2 adsorption and desorption isotherms were determined on a Micromeritics TRISTAR 3000 sorptometer at −196 °C. The mesopore pore size distribution was determined by the BJH (Barrett, Joyner, Halenda) method applied to the adsorption branch of the isotherm. Mercury intrusion porosimetry measurements were performed on Micromeritics AutoPore IV. Macropore size distribution was obtained by applying the Washburn equation to the mercury intrusion curves. Fourier transform infrared (FT-IR) spectra were recorded using a IRAffinity-1 spectrometer (Shimadzu) in the transmission and attenuated total reflection (ATR) mode. Dynamic light scattering (DLS) experiments and zeta-potential value analyses were performed with a Malvern 300HSA Zetasizer instrument.

Drug partitioning ratio

To determine the drug partitioning between the lipid core and the micellar phase, 1 mL CU-NHP-SLN dispersion was added to ethanol in order to precipitate NHP, and then the sample was centrifuged at 5000 rpm for 5 min. The precipitate was further washed with 20 mL water 2 times and dried at 40 °C for 7 days. 10 mg of the dried SLN precipitate was dissolved in 25 mL methylene chloride and then analyzed by UV spectrometry (UV-Visible CARY3E-Varian, USA) at 423 nm and its concentration was calculated using a standard curve of curcumin in methylene chloride. In the case of CU-SA-SLNs, 1 mL SLN dispersion was filtered using a Millipore membrane (0.20 μm). The filtrate was then washed with water (2 × 20 mL) and further dried at 40 °C for 7 days. 10 mg of the filtrate was analyzed by the same method used for CU-NHP-SLNs. The entire amount of curcumin initially added into SLN dispersions (1 mg/100 mg lipid/100 mg silica) was recovered by extraction with dichloromethane from the hybrid silica material, as it was quantified by UV spectrometry. The partitioning ratio was calculated by dividing the analyzed weight of curcumin in dried lipid to the

total weight of curcumin in the SLN formulation. All data reported are the mean ± standard deviation of at least three different experiments.

In vitro drug release experiments

Release experiments were carried out under sink conditions by dispersing 100 mg of the hybrid material (0.406 mg of curcumin) in 50 mL of buffered receiving solution that contains 0.1 wt% of CTAB.[28] The system was maintained at 25 °C under magnetic stirring at 100 rpm. The pH of the receiving solution was adjusted to obtain various values, 1.2, 4.5 and 7.4. At regular intervals, 1.5 mL aliquots were withdrawn and replaced by an equal volume of receiving solution. The withdrawn samples were centrifuged at 5000 rpm for 5 min and the supernatants were diluted with the initial receiving medium and filtered on a 0.45 μm membrane filter (Acrodisc Syringe Filger). The released curcumin was analyzed using a UV spectrometer at 423 nm and its concentration was calculated using a standard curve of curcumin established for each dissolution medium. The cumulative release percentage was calculated using a dilution factor correction. All data reported are the mean ± standard deviation of at least three different experiments.

Results and discussion

Curcumin loading into solid lipid nanoparticles

Curcumin-loaded solid lipid nanoparticles (CU-Lipid-SLNs), used as both a macro-template for the silica material and a reservoir of curcumin, were prepared by sonicating a hot emulsion containing the melted lipid (NHP or SA) and micelles of Pluronic P123. This consists of a first molten lipid/water emulsion method using a biocompatible surfactant as a stabilizer. Dynamic light scattering (DLS) measurements showed that there was a slight increase in mean diameters for curcumin-loaded SLNs, compared to those of blank SLNs (Table 1). Zeta potential measurements give slightly negative values (around −10 mV), which are consistent with molecularly organized systems of non-ionic surfactants (here micelles of P123) that might adsorb at the water–SLN interface to stabilize the dispersions.[29] The absolute values of the zeta potential are slightly higher for blank-SA-SLNs than for blank-NHP-SLNs, probably due to the presence of small amounts of stearate in the P123 layer stabilizing the nanoparticles. However, the zeta potential value does not show a significant change for drug-loaded SLNs, thus suggesting that the interface of the solid nanoparticles were not affected by the curcumin loading.

Table 1 Physicochemical characteristics of SLNs[a]

SLN formulation	MD (nm)	ZP (mV)	PR (%)
Blank-NHP-SLNs	292 ± 35	−11.0 ± 1.4	—
CU-NHP-SLNs	313 ± 43	−8.2 ± 2.1	20 ± 3
Blank-SA-SLNs	426 ± 38	−16.0 ± 1.4	—
CU-SA-SLNs	447 ± 44	−15.1 ± 1.1	65 ± 5

[a] MD: mean diameter, ZP: zeta potential, PR: partitioning ratio.

The drug partitioning ratio (PR) between the lipid core of SLNs and the micelles depends on the lipid source. For CU-NHP-SLNs, about 80 wt% of CU is dispersed in the micellar phase which means that only 20% of the curcumin is in the lipid core.

The PR for CU-SA-SLNs increased drastically up to 65%, probably due to the better interaction between SA and curcumin, as it was further confirmed by FT-IR spectra. Indeed, according to FT-IR spectra for CU-Lipid-SLNs and pure lipids (Fig. 1A), no shift of the ν_{CO} bond of NHP was observed when adding CU (CU-NHP-SLN), while a more pronounced peak at 1681 cm^{-1} appeared for SA (CU-SA-SLNs). This could be assigned to a ν_{CO} of the SA forming a hydrogen bond with the enol form of CU (Fig. 1Aa and b), while for CU-NHP-SLNs no peak appeared after encapsulation of curcumin (Fig. 1Ac and d).

SAXS experiments also confirmed SA–curcumin interactions (Fig. 1B, ESI† for full SAXS spectra). After encapsulation of CU in SLNs based on SA (CU-SA-SLNs), the position of the (001)-reflection is slightly shifted to a lower q value compared to blank SA-SLNs[30] (Fig. 1B). This shift might be caused by the interaction between curcumin and stearic acid that was shown in FT-IR. For CU-NHP-SLNs, the shift is not visible, probably due to the lack of interaction between NHP and CU. Therefore, it is reasonable to assume that the encapsulation rate into the lipid core of CU-SA-SLN could be enhanced by hydrogen bonding.[31]

Characterization of silica materials

Curcumin-loaded SLN dispersions were silicified into meso- and macro-compartmentalized hybrid materials, following a procedure previously reported.[13] Herein this procedure was extended to stearic acid and to curcumin-loaded nanoparticles, based on NHP and SA, respectively. Silicalization occurs through a dual templating mechanism combining self-assembling of micelles into mesostructured domains[32] and transcription of lipid nanoparticles into macro-structured domains. Curcumin loading and the nature of the solid lipid (NHP or SA) did not significantly affect the meso-structuring of the silica materials. Bare silica was obtained by removing organic matter by soxhlet extraction with ethanol for 48 h. To investigate the mesostructuring of the silica materials, the small angle X-ray

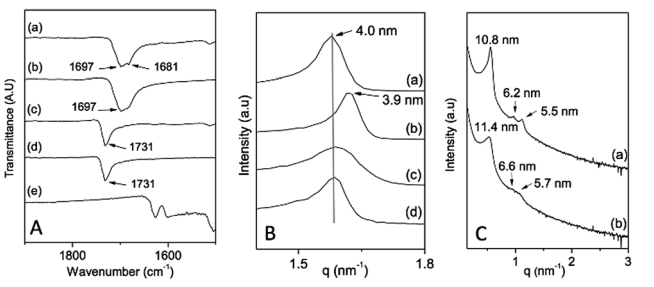

Fig. 1 IR spectra (A) and SAXS pattern (B) of CU-SA-SLNs (a), blank-SA-SLNs (b), blank-NHP-SLNs (c), CU-NHP-SLNs (d), curcumin (e); SAXS pattern (C) of NHP-Mat (a) and SA-Mat (b) after removal of organic matter. Values in SAXS patterns represent Bragg distances $d = 2\pi/q$, where q is the scattering vector.

scattering (SAXS) experiment was carried out. The SAXS data for bare NHP-Mat (Fig. 1Ca), indicate 3 peaks, which can be attributed to the (100), (110) and (200) reflections of the hexagonal structure. In the case of bare SA-Mat (Fig. 1Cb), the second and the third peak, which correspond to (110) and (200) reflections of the hexagonal structure, were less resolved than NHP-Mat. The lattice parameters, $a_0 = 2d_{100}/\sqrt{3}$, are calculated as 12.5 nm and 13.2 nm for NHP-Mat and SA-Mat.

N_2 adsorption–desorption isotherms for bare silica materials are shown in Fig. 2. According to these graphs, both samples exhibit a type IV isotherm and the specific surface area and pore volume values are 794 $m^2\ g^{-1}$ and 0.8 $cm^3\ g^{-1}$ for NHP-Mat, 943 $m^2\ g^{-1}$ and 1.2 $cm^3\ g^{-1}$ for SA-Mat, respectively. The pore diameter distribution is narrow and centered at 6.8 nm and 6.0 nm for NHP-Mat and SA-Mat. The wall thickness, deduced by subtracting the pore diameter from the lattice parameter a_0, is equal to 5.7 nm and 7.2 nm for NHP-Mat and SA-Mat. These values are higher than those of SBA-15 (4 nm), which means that these silica materials could be more stable than the conventional SBA-15.[33]

Imprint of SLN beads on silica materials was confirmed by mercury intrusion porosimetry measurements on bare materials. In Fig. 3A, a broad peak centered at 900 nm is observed for NHP-Mat. These macropores, generated by CU-NHP-SLN, are larger than the mean diameter of CU-NHP-SLN, which is around 310 nm. This is probably due to the possible aggregation of NHP during mineralization by TMOS, in which hydrothermal treatment was conducted at 70 °C, above the melting point of NHP (54 °C). For SA-Mat (Fig. 3B), the peak corresponding to macropores is centered at 470 nm that is almost identical to the size of CU-SA-SLN beads (450 nm). This could be explained by the fact that nanoparticles of stearic acid with a melting point of 68 °C remain solid and do not change their shape under hydrothermal treatment at 70 °C.

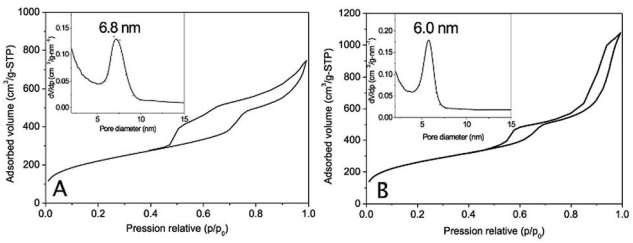

Fig. 2 Nitrogen adsorption–desorption isotherms and pore size distribution (inset) of NHP-Mat (A) and SA-Mat (B).

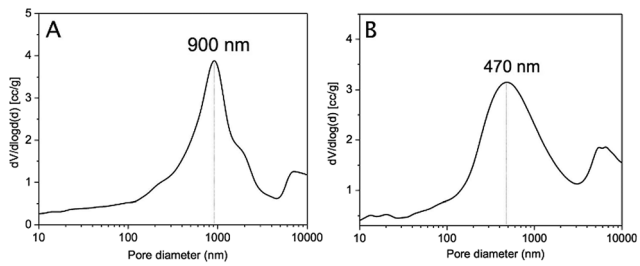

Fig. 3 Macropore size distribution of NHP-Mat (A) and SA-Mat (B).

Clear evidence of macroporosity can be obtained by the morphology studies of these materials using SEM (Fig. 4).

Transmission electron microscopy (TEM) was performed for these materials to visualize macropore and mesopore structures. Macropores are observed for both NHP-Mat (Fig. 5A and B) and SA-Mat (Fig. 5C and D) and their diameters are in agreement with porosimetry measurements, proving once again that the imprints of macropores by SLNs have been successfully achieved for both materials. Also, TEM analysis allows us to observe the mesoporosity of these samples, whose diameter is around 6 nm, as calculated by the N_2 adsorption–desorption isotherm.

In vitro drug release

The release experiments of CU-loaded hybrid SLN silica materials were carried out in 3 different dissolution media (pH 1.2, 4.5 and 7.4).

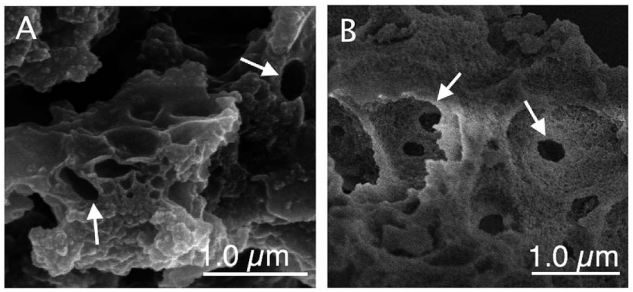

Fig. 4 SEM image of meso–macroporous silica NHP-Mat (A) and SA-Mat (B) after removal of organic matter (arrows indicate marcopores).

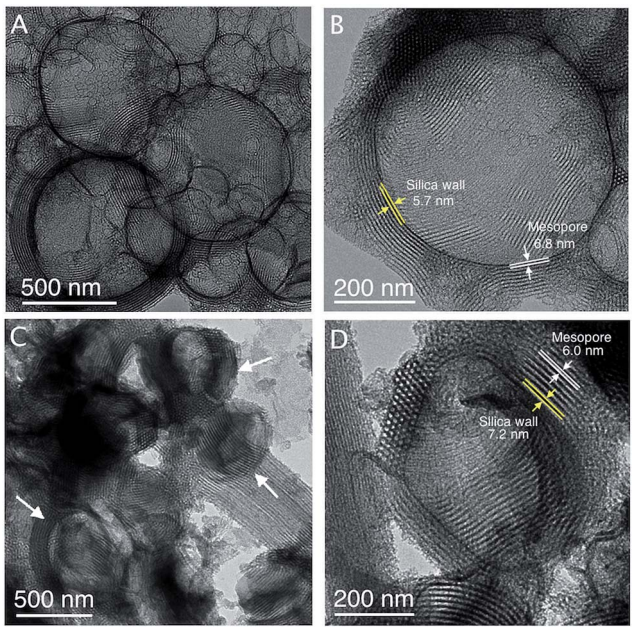

Fig. 5 TEM image of meso–macroporous silica NHP-Mat (A and B) and SA-Mat (C and D) after removal of organic matter (arrows indicate marcopores).

CTAB, 0.1% (w/w), was added to dissolution media in order to solubilize the curcumin,[34] because curcumin is poorly soluble and degraded in aqueous solution.[35] Before investigating curcumin release, the stability of curcumin for 5 days and the sink conditions in different dissolution media were verified (less than 1% loss).

Fig. 6 and 7 show the cumulative release of curcumin from hybrid materials at 25 °C at different pH release media. At first, the drug released from NHP-Mat (Fig. 6) quickly reached the plateau within 6 h at any pH. However, the maximum cumulative release percentage was varied according to the pH, 100%, 88%, and 16% for pH 1.2, 4.5 and 7.4, respectively.

The differences in the curcumin release behavior might be due to the interaction between curcumin and silanol groups at the surface of silica. One should first note that no deprotonated forms of curcumin are involved in the release mechanism at the investigated pH (1.2, 4.5 and 7.4) since pK_a of the most acidic proton is 8.4 (Fig. 9). Secondly, through a well-known isoelectric point the value for amorphous silica in water is 2–3,[36] which is based on pK_{a1} = −2.77 ($\equiv SiOH_2^+ \rightarrow \equiv SiOH + H^+$) and p$K_{a2}$ = 6.77 ($\equiv SiOH \rightarrow \equiv SiO^- + H^+$), for calculation of surface acidity in mesoporous silica, protonation–deprotonation reaction for Q^2 silanol ($=Si(OH)_2$) and Q^3 silanol ($\equiv$Si–OH) should be also be taken into consideration.[37] Experimental data[38] and computational calculations[39] suggested that Q^3 silanol on the silica surface has a pK_a of 4.5 and Q^2 silanol has a pK_a of 8.5.

Therefore, in the 1.2–7.4 pH interval only Q^3 silanol undergoes deprotonation, while Q^2 silanol is not deprotonated. These dominated forms of silica and curcumin as a function of pH are described in Fig. 8. At pH 1.2, only weak dipole–dipole interactions (hydrogen bond, 5.0 kcal mol^{-1}, computational calculation[40]) between curcumin and silanol are expected. Those are not strong enough to hold the curcumin inside mesopores and therefore the release kinetics are the highest (Fig. 9a). At pH 4.5, where pH = pK_a of $\equiv$Si–OH, as half of Q^3 silanol is protonated, it becomes more effective to hold curcumin than at pH 1.2 (Fig. 9b). Finally, when pH increases to 7.4, all Q^3 silanols are deprotonated, being the most effective to hold curcumin *via* stronger ion–dipole interactions (23 kcal mol^{-1} (ref. 40)) (Fig. 9c).

CU release from SA-Mat (Fig. 7) show also the pH dependent release pattern (CU cumulative release: 86, 68 and 18% for pH 1.2, 4.5 and 7.4, respectively). However, the release rate is slower than that of NHP-Mat (12 h *vs.* 6 h for saturation). It could be related to a higher amount of curcumin into the lipid core and to the lipid–curcumin interaction for SA-Mat. Indeed, after CU release that is encapsulated in mesopores, CU is fed only from the SLN that acts as a drug reservoir. Hence, the release rate

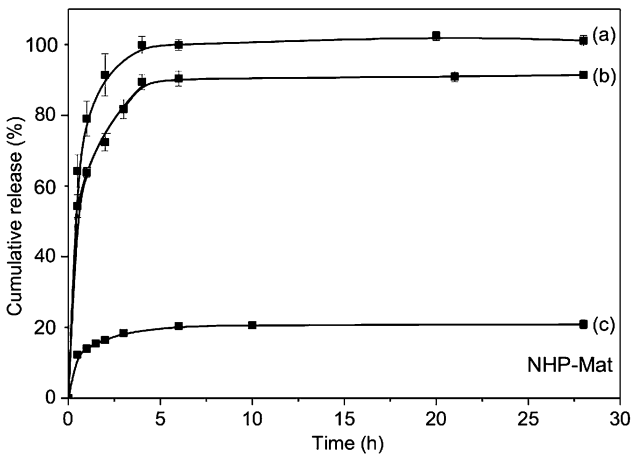

Fig. 6 Curcumin cumulative release from NHP-Mat (a) at pH 1.2, (b) at pH 4.5 and (c) at pH 7.4.

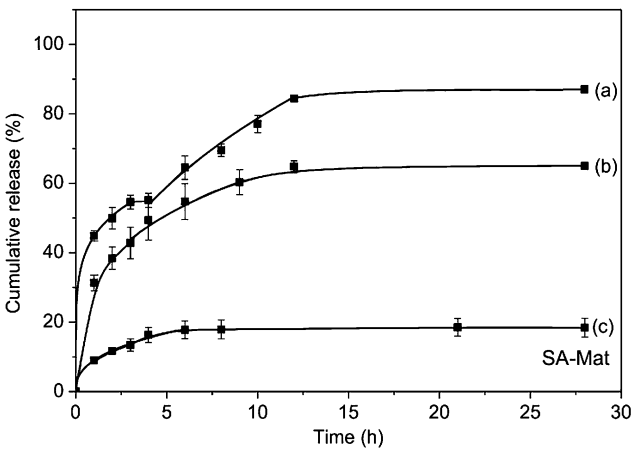

Fig. 7 Curcumin cumulative release from SA-Mat (a) at pH 1.2, (b) at pH 4.5 and (c) at pH 7.4.

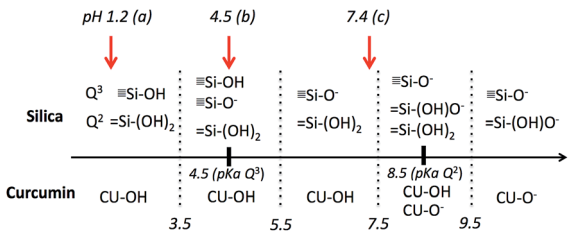

Fig. 8 Dominant forms of silica and CU as a function of pH.

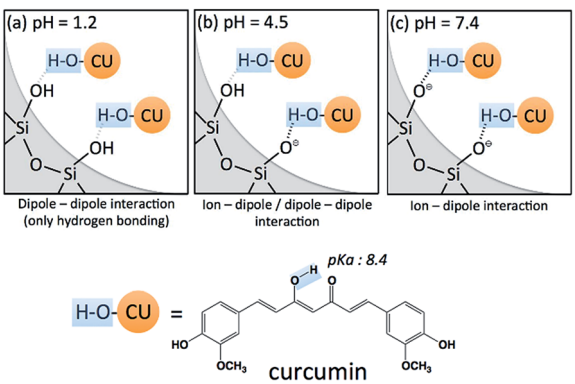

Fig. 9 Possible interactions between curcumin and silanol on a silica surface (a) at pH 1.2, (b) at pH 4.5 and (c) at pH 7.4.

becomes mainly dependent on the nature of SLN, which is again, influenced by pH.[41] Interestingly, at pH 1.2, a two-step release pattern was observed with the quasi-stationary state between 3 h and 4 h (Fig. 7a). This state will be discussed below using a kinetic model. The presence of this quasi-stationary state was verified more than 10 times.

Drug release mechanism modeling

In order to determine the release mechanism, the data were analysed and fitted using the Korsmeyer–Peppas model[42] (Table 2). It was revealed that in all cases, the drug release mechanism could be described by the quasi-Fickian drug diffusion process, since all release exponent (n) values are lower than 0.43 (see SI3† for fitting graphs). The kinetic constants of NHP-Mat are about two times higher than those of SA-Mat, which confirms also our suggestion considering the interaction between the lipid and CU.

However, the release pattern for SA-Mat at pH 1.2 was not well fitted using the Korsmeyer–Peppas model. It is probably due to the difference of the CU release rate from SLNs and mesopores. As explained, CU release at pH 1.2 is faster than at other pHs, and CU release from mesopores is faster than CU from SLNs. As a result, at pH 1.2 CU release from mesopores of SA-Mat finished in 3 h (Fig. 7a), while CU release from SLN have not started yet. The Korsmeyer–Peppas model fitting on 2 zones can confirm this two-step release. At first, it is clearly shown that the value of the correlation coefficient R^2 for both the 1st zone (0.990 before 3 h) and the 2nd zone (0.992 after 4 h) are close to 1, which supports a two-step release hypothesis. In addition, the kinetic constant for the 1st zone (44.6 h^{-1}) is higher than that for the 2nd zone (33.4 h^{-1}), which explains fast CU release from mesopores, compared to SLNs.

Moreover, the disappearance of stearic acid from SA-Mat over the release time was also confirmed by SAXS measurements (Fig. 10B). Like in FT-IR experiments (Fig. 10A), the continuous decrease of the peak corresponding to stearic acid is observed at pH 1.2 (a–c) while this peak remains at pH 7.4 even after 6 h release (d).

A possible mechanism of the core–shell bionanohybrid vectors described is schematized in Fig. 11.

Considering the toxicity of designed vectors, it should be noted that all ingredients are excipient approved by the FDA,[25] except NHP. Thus, for NHP-based formulations, cell viability experiments were performed on MRC-5 cells (Fig. SI5†) following a standard procedure previously reported (see ESI†).[43]

Table 2 Release kinetic parameters[a]

	NHP-Mat			SA-Mat		
Parameter	pH 1.2	pH 4.5	pH 7.4	pH 1.2	pH 4.5	pH 7.4
K (h^{-1})	76.6	63.4	14.2	42.4	31.4	8.9
R^2	0.969	0.991	0.993	0.950	0.994	0.982
N	0.212	0.233	0.211	0.250	0.299	0.411

[a] K: release rate constant, R^2: correlation coefficient, n: release exponent.

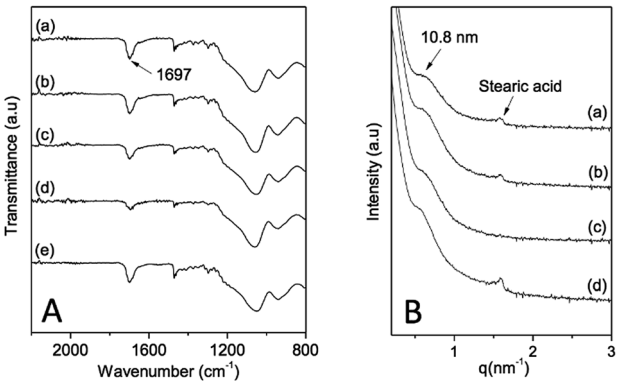

Fig. 10 FT-IR (A) spectra of SA-Mat (a) as-synthesized material, (b) after 2 h release at pH 1.2, (c) after 4 h release at pH 1.2, (d) after 8 h release at pH 1.2, (e) after 6 h release at pH 7.4; SAXS patterns (B) of SA-Mat (a) after 2 h release at pH 1.2, (b) after 4 h release at pH 1.2 (c) after 8 h release at pH 1.2 (d) after 6 h release at pH 7.4.

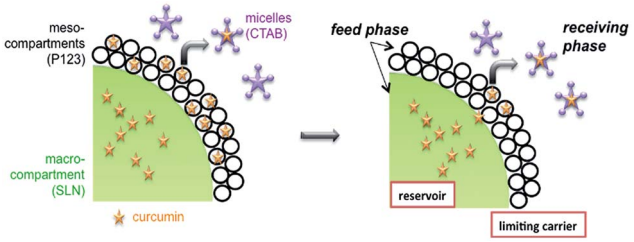

Fig. 11 Graphical representation of the release mechanism of curcumin from core–shell SLN/mesoporous silica.

Indeed, the determined IC_{50} values of free curcumin and CU-NHP-Mat were identical after 24 h of treatment, of about 20 mg L^{-1} of curcumin in both cases and of about 4.9 g L^{-1} of NHP–silica in the case of CU-NHP-Mat. At the same concentration in NHP–silica, free of curcumin material NHP-Mat, 90% of the cells remained viable. These results confirm that NHP, silica, and P123 surfactants were not toxic below this dose. As a matter of fact, the IC_{50} value of NHP-Mat is higher than 18 g L^{-1}. Thus the newly designed drug-SLN-silica meso–macro-compartmentalized silica matrix could be of potential interest for biological applications, including drug delivery.

Conclusions

Curcumin-loaded meso–macrostructured silica materials were obtained by mineralizing dispersions of solid lipid nanoparticles in micellar solutions. The partition of curcumin between SLNs and micelles of P123 depends on the lipid source (20% for NHP and 65% for SA). The release of curcumin is pH-dependent for both stearic acid and cetyl palmitate-based materials, probably due to the interaction between CU and silanols of the mesopore surface. Moreover, a two-step release pattern was observed for SA-Mat at pH 1.2, as confirmed by FT-IR and SAXS analysis. This result suggests that SLNs may act as reservoirs of curcumin (CU), while mesopores act as

pathways to control drug release. In conclusion, using SLN/micellar dispersion is a straightforward way to design a novel hybrid-silica drug delivery system with improved stability and sustainability of guest drug release.

Acknowledgements

The authors would like to thank Mélanie Emo for performing the X-ray measurements, Jaafar Ghanbaja and Emmanuel Lamouroux for TEM facilities. Authors acknowledge Raphael E. Duval and Stéphane Fontanay for useful discussions and for assistance in performing cell viability measurements.

Notes and references

1 K. Loomis, K. McNeeley and R. V. Bellamkonda, *Soft Matter*, 2011, **7**, 839; K. Raemdonck, K. Braeckmans, J. Demeestera and S. C. De Smedt, *Chem. Soc. Rev.*, 2014, **43**, 444; M. Elsabahy and K. L. Wooley, *Chem. Soc. Rev.*, 2012, **41**, 2545; V. Biju, *Chem. Soc. Rev.*, 2014, **43**, 744.

2 M. Vallet-Regi, A. Raamila, R. P. del Real and J. Perez-Pariente, *Chem. Mater.*, 2001, **13**, 308.

3 B. Munoz, A. Ramila, J. Perez-Pariente, I. Díaz and M. Vallet-Regí, *Chem. Mater.*, 2003, **15**, 500; P. Yang, S. Gaib and J. Lin, *Chem. Soc. Rev.*, 2012, **41**, 3679; V. Mamaeva, C. Sahlgren and M. Linden, *Adv. Drug Delivery Rev.*, 2013, **65**, 689; C. Argyo, V. Weiss, C. Braüchle and T. Bein, *Chem. Mater.*, 2014, **26**, 435.

4 Complementary Medicine Evaluation Committee extracted ratified minutes, sixteenth meeting, 1999; H. Zhang, D. R. Dunphy, X. Jiang, H. Meng, B. Sun, D. Tarn, M. Xue, X. Wang, S. Lin, Z. Ji, R. Li, F. L. Garcia, J. Yang, M. L. Kirk, T. Xia, J. I. Zink, A. Nel and C. J. Brinker, *J. Am. Chem. Soc.*, 2012, **134**, 15790.

5 F. Balas, M. Manzano, P. Horcajada and M. Vallet-Regi, *J. Am. Chem. Soc.*, 2006, **128**, 8116.

6 H. Zheng, Y. Wang and S. Che, *J. Phys. Chem. C*, 2011, **115**, 16803; S. H. Cheng, W. N. Liao, L. M. Chen and C. H. Lee, *J. Mater. Chem.*, 2011, **21**, 7130; J. E. Lee, D. J. Lee, N. Lee, B. H. Kim, S. H. Choi and T. Hyeon, *J. Mater. Chem.*, 2011, **21**, 16869.

7 E. Aznar, L. Mondragon, J. V. Ros-Lis, F. Sancenon, M. D. Marcos, R. Martínez-Manez, J. Soto, E. Perez-Paya and P. Amoros, *Angew. Chem., Int. Ed.*, 2011, **50**, 11172; A. Schlossbauer, S. Warncke, P. M. E. Gramlich, J. Kecht, A. Manetto, T. Carell and T. Bein, *Angew. Chem., Int. Ed.*, 2010, **49**, 4734.

8 W. Zhao, J. Gu, L. Zhang, H. Chen and J. Shi, *J. Am. Chem. Soc.*, 2005, **127**, 8916; S. Huang, P. Yang, Z. Cheng, C. Li, Y. Fan, D. Kong and J. Lin, *J. Phys. Chem. C*, 2008, **112**, 7130.

9 Y. Zhang, Z. Zhi, T. Jiang, J. Zhang, Z. Wang and S. Wang, *J. Controlled Release*, 2010, **145**, 257; X. Kang, Z. Cheng, D. Yang, P. Ma, M. Shang, C. Peng, Y. Dai and J. Lin, *Adv. Funct. Mater.*, 2012, **22**, 1470.

10 N. W. Clifford, K. S. Iyer and C. L. Raston, *J. Mater. Chem.*, 2008, **18**, 162; S. F. Chin, K. S. Iyer, M. Saunders, T. G. St. Pierre, C. Buckley, M. Paskevicius and C. L. Raston, *Chem.–Eur. J.*, 2009, **15**, 5661.

11 P. Botella, A. Corma and M. Quesada, *J. Mater. Chem.*, 2012, **22**, 6394.

12 S. Das and A. Chaudhury, *AAPS PharmSciTech*, 2011, **12**, 62; R. H. Müller, K. Mäder and S. Gohla, *Eur. J. Pharm. Biopharm.*, 2000, **50**, 161.

13 A. Pasc, J. L. Blin, M. J. Stébé and J. Ghanbaja, *RSC Adv.*, 2011, **1**, 1204; R. Ravetti-Duran, J. L. Blin, M. J. Stebe, C. Castel and A. Pasc, *J. Mater. Chem.*, 2012, **22**, 21540.

14 H. P. Ammon and M. A. Wahl, *Planta Med.*, 1991, **57**, 1.

15 B. B. Aggarwal and K. B. Harikumar, *Int. J. Biochem. Cell Biol.*, 2009, **41**, 40; J. S. Jurenka, *Alternative Med. Rev.*, 2009, **14**, 141; R. K. Maheshwari, A. K. Singh, J. Gaddipati and R. C. Srimal, *Life Sci.*, 2006, **78**, 2081; M. M. Yallapu, M. Jaggi and S. C. Chauhan, *Drug Discovery Today*, 2012, **17**, 71.

16 B. B. Aggarwal, A. Kumar and A. C. Bharti, *Anticancer Res.*, 2003, **23**, 363.

17 J. A. Bush, K. J. Cheung Jr and G. Li, *Exp. Cell Res.*, 2001, **271**, 305.

18 J. K. Lin, M. H. Pan and S. Y. Lin-Shiau, *Biofactors*, 2000, **13**, 153.

19 E. Pfeiffer, S. Hohle, A. M. Solyom and M. Metzler, *J. Food Eng.*, 2003, **56**, 257.

20 P. Anand, A. B. Kunnumakkara, R. A. Newman and B. B. Aggarwal, *Mol. Pharm.*, 2007, **4**, 807.

21 D. Chirio, M. Gallarate, M. Trotta, M. E. Carlotti, E. Calcio Gaudino and G. Cravotto, *J. Inclusion Phenom. Macrocyclic Chem.*, 2009, **65**, 391.

22 S. Jambhrukar, S. Karmakar, A. Popat, M. Yu and C. Yu, *RSC Adv.*, 2014, **4**, 709.

23 W. Tiyaboonchai, W. Tungpradit and P. Plianbangchang, *Int. J. Pharm.*, 2007, **337**, 299.

24 B. Heurtault, P. Saulnier, B. Pech, J. E. Proust and J. P. Benoit, *Biomaterials*, 2003, **24**, 4283.

25 http://www.accessdata.fda.gov/scripts/cder/iig/index.Cfm.

26 D. Sutaria, B. K. Grandhi, A. Thakkar, J. Wang and S. Prabhu, *Int. J. Oncol.*, 2012, **41**, 2260.

27 N. Canilho, A. Pasc, M. Emo, M.-J. Stébé and J.-L. Blin, *Soft Matter*, 2013, **9**, 10832.

28 M. H. M. Leung, H. Colangelo and T. W. Kee, *Langmuir*, 2008, **24**, 5672; Y. J. Wang, M. H. Pan, A. L. Cheng, L. I. Lin, Y. S. Ho, C. Y. Hsieh and J. K. Lin, *J. Pharm. Biomed. Anal.*, 1997, **15**, 1867.

29 A. P. Nayak, W. Tiyaboonchai, S. Patankar, B. Madhusudhan and E. B. Souto, *Colloids Surf., B*, 2010, **81**, 263; L. Hu, X. Tang and F. Cui, *J. Pharm. Pharmacol.*, 2004, **56**, 1527.

30 S. M. Martins, B. Sarmento, C. Nunes, M. Lucio, S. Reis and D. C. Ferreira, *Eur. J. Pharm. Biopharm.*, 2013, **85**, 488.

31 R. H. Muller, S. A. Runge, V. Ravelli, A. F. Thunemann, W. Mehnert and E. B. Souto, *Eur. J. Pharm. Biopharm.*, 2008, **68**, 535.

32 Q. Huo, D. I. Margolese and G. D. Stucky, *Chem. Mater.*, 1996, **8**, 1147.

33 D. Zhao, J. Feng, Q. Huo, N. Melosh, G. H. Fredrickson, B. F. Chmelka and G. D. Stucky, *Sciences*, 1998, **279**, 548.

34 D. Ke, X. Wang, Q. Yang, Y. Niu, S. Chai, Z. Chen, X. An and W. Shen, *Langmuir*, 2011, **27**, 14112.
35 Z. Wang, M. H. M. Leung, T. W. Kee and D. S. English, *Langmuir*, 2010, **26**, 5520.
36 R. K. Iler, *The Chemistry of Silica*, Wiley, New York, 1979.
37 S. Ong, X. Zhao and K. B. Eisenthal, *Chem. Phys. Lett.*, 1992, **191**, 327.
38 P. Schindler and H. R. Kamber, *Helv. Chim. Acta*, 1968, **51**, 1781; J. M. Rosenholm, T. Czuryszkiewicz, F. Kleitz, J. B. Rosenholm and M. Linden, *Langmuir*, 2007, **23**, 4315; J. P. O'Reilly, C. P. Butts, I. A. I'Anson and A. M. Shaw, *J. Am. Chem. Soc.*, 2005, **127**, 1632.
39 K. Leung, I. M. B. Nielsen and L. J. Criscenti, *J. Am. Chem. Soc.*, 2009, **131**, 18358.
40 T. Steiner, *Angew. Chem., Int. Ed.*, 2002, **41**, 49; S. Gronert, *J. Am. Chem. Soc.*, 1993, **115**, 10258; Y. Gu, T. Kar and S. Scheiner, *J. Am. Chem. Soc.*, 1999, **121**, 9411.
41 E. Zimmermann and R. H. Muller, *Eur. J. Pharm. Biopharm.*, 2001, **52**, 203.
42 P. Costa and J. M. Sousa Lobo, *Eur. J. Pharm. Sci.*, 2001, **13**, 123.
43 T. Mosmann, *J. Immunol. Methods*, 1983, **65**, 55; M. Grare, M. Mourer, S. Fontanay, J. B. Regnouf-de-Vains, C. Finance and R. E. Duval, *J. Antimicrob. Chemother.*, 2007, **60**, 575.